Transient Electro-osmotic Pumping in Rectangular Microchannels

Gholamreza Karimi and J. Richard Culham
Microelectronics Heat Transfer Laboratory
Department of Mechanical Engineering
University of Waterloo, Waterloo, Ontario, N2L 3G1, Canada
karimir@mhtlab.uwaterloo.ca
rix@mhtlab.uwaterloo.ca

Abstract

Two-dimensional Poisson-Boltzmann and momentum equations are solved simultaneously to study the transient characteristics of electro-osmotic pumping in a rectangular microchannel. A finite difference scheme with variable grid spacing is used to calculate electric potential distribution. Time variations of velocity profiles are obtained by using a combined ADI-TDMA technique.

Numerical solutions show significant influences of the channel hydraulic diameter, the aspect ratio, and the applied voltage on the transient and steady state velocity fields and the resulting volumetric flow rates. As the channel hydraulic diameter is increased, it takes a longer period for the flow to reach steady state condition. On the other hand, as the channel aspect ratio deviates from the square, a steady-state flow field is reached in a shorter period, and a slightly larger flow can be obtained. The numerical results also show that the steady state channel throughput is linearly increasing with the applied voltage along the channel length.

1. Introduction

Recent developments in microfabrication technologies have enabled a variety of miniaturized fluidic systems capable of performing various chemical and biological analyses for medical, pharmaceutical, defense, and environmental monitoring applications. Compared to their conventional counterparts, microscale devices offer higher throughput, shorter processing/analysis times, reduced sample volumes, the possibility of in situ operations, and reduced operation and manufacturing costs.

Over the past decade, microfluidic systems have received growing attractions particularly in drug delivery applications, DNA analysis/sequencing systems, microscale biological and chemical agent detection sensors, microreactors for the analysis of biological cells, and cooling of microelectronic systems.

Along with the necessary sensors and electronic units, microfluidic systems consist of various fluid handling components such as microchannels, pumps, and valves. Given the small scales involved with these systems, there are some shortcomings to conventional mechanical fluid propulsion systems. For instance, microscale pumps have small moving parts which are difficult to manufacture and repair. A non-mechanical alternative for moving liquids in microchannels is electro-osmotic pumping, which takes advantage of the electrical properties of the liquid to induce flow. Electro-osmosis has a strong potential for use in microfluidic systems in which liquid pumping, handling, and control can be achieved through selective applications of electric fields, eliminating moving mechanical devices such as valves and flow switches.

Probably the most important issue concerning electro-osmotic pumping is its direct dependence on the applied voltage. A high efficiency electro-osmotic pumping is achieved at high electric fields. As the electric field strength is increased the system reliability will degrade primarily due to an increase in the system power consumption, safety considerations, and the associated elevated solution temperature (Joulean heating) as mentioned by Gad-el-Hak, 2002 [6]. However, electro-osmotic pumping is still an excellent choice for microfluidic systems operating at very small flow rates such as lab-on-a-chip systems. In these cases, it is more effective if the liquid handling or drug delivery is carried out precisely according to a predefined time-dependent pattern. On the other hand, more useful therapies can be achieved by adjusting the drug injection with time and eliminating the potential for both under- and overdosing.

The majority of the recently published papers studied electro-osmotic pumping under steady-state conditions. However, it will be very useful to investigate the flow handling performance of such systems under transient condi-

tions.

Motivated by the advances in fluid handling devices with nonmoving components, the present study will address the electro-osmotic driven flows in straight two-dimensional channels under transient conditions. This paper is organized as follows: first, the governing equations for the electro-osmotic potential distribution will be presented. Next, the governing equations for transient flow in a rectangular microchannel and the numerical solution techniques will be given. Finally, the effect of different design and operating parameters on the pumping efficiency and transient behavior of the electro-osmotic pumping will be presented and discussed.

2. Governing Equations

2.1. Electric Double Layer (EDL) and Electro-osmosis

Most solid surfaces obtain a surface electric charge when they are brought into contact with a polar liquid (electrolyte). This may be due to ionization, ion adsorption or ion dissolution [7]. The surface charges, in turn, influence the ion distribution in the electrolyte. This phenomenon is illustrated in Fig. 1. As seen in this figure, the attraction from the negative wall causes some of the positive ions (so called counter-ions) to cluster immediately near the wall forming a firm layer around the surface. This layer is known as the Stern layer and has a typical thickness of one ionic diameter. The ions within the Stern layer are attracted firmly to the wall with strong electrostatic forces and are practically immobile. Additional positive ions are still attracted by the negative wall however, they are repelled by the Stern layer as well as by other positive ions that are also competing to approach the wall. This dynamic equilibrium results in the formation of a Gouy-Chapman diffuse layer of counter-ions where the concentration near the wall is at the highest and decreases gradually with distance until it reaches equilibrium with the counter-ion concentration in the bulk solution [1]. The ions in this region are free and available to impart work on the fluid. The plane separating the Stern and Gouy-Chapman layers is called the shear plane. Likewise, the concentration of the negative ions (co-ions) gradually increases with distance as the repulsive forces of the wall are screened out by the positive ions, until equilibrium is again reached.

The combination of the attached counter-ions in the Stern layer and the charged region near the surface referred to as the Electric Double Layer, EDL, exists in a very narrow region close to the wall. Within the EDL, counter-ions and co-ions are preferentially distributed, such that the net charge density is nonzero. The resulting electric potential is maximum at the wall, drops rapidly through the Stern layer, and gradually diminishes toward zero as the concentration of positive and negative ions merge together at farther distances (Fig. 1). The potential at the shear plane, which is also the boundary of the fluid flow problem, is called the zeta potential, ζ. Because of the difficulties associated with predicting the properties of the Stern layer, the ζ potential is typically determined empirically from electro-osmotic or streaming potential flow measurements [7].

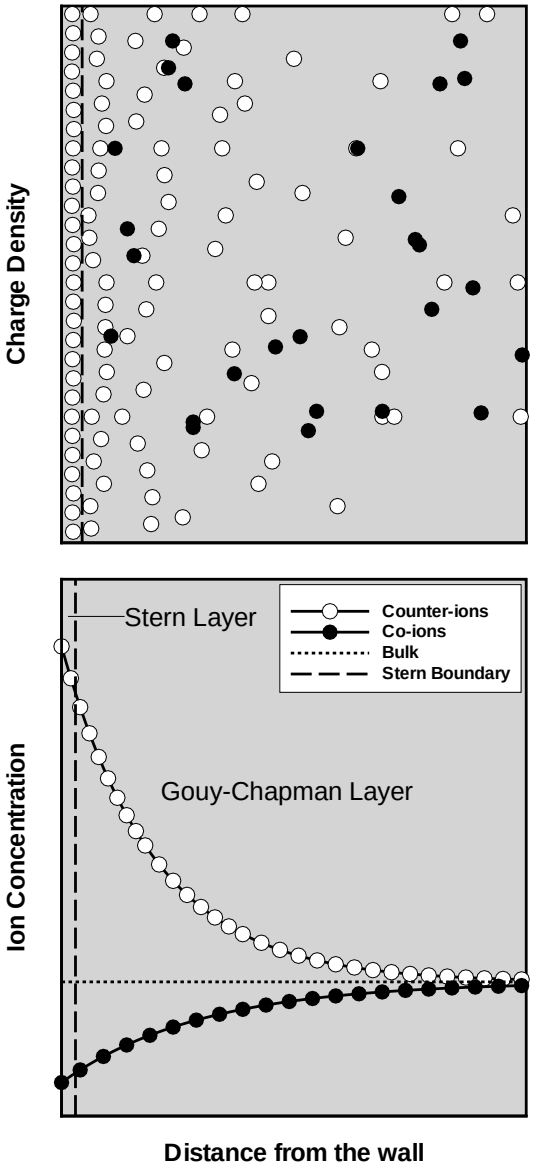

Figure 1. Charge density and ion concentration distributions in a typical EDL

If an electric field is applied along the length of the channel, an electrokinetic body force is exerted on the ions in the

diffuse layer of the EDL. The ions will move under the influence of the applied electrical field, pulling the liquid with them and resulting in electro-osmotic flow as illustrated in Fig. 2. The fluid movement is carried through to the rest of the fluid in the channel by viscous forces. This phenomenon is called electro-osmosis.

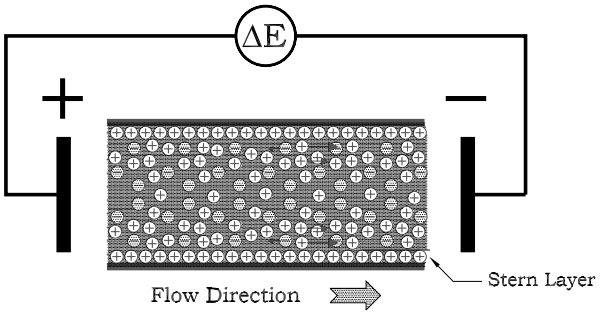

Figure 2. Electrokinetic body force acting on a polar liquid

The electrokinetic effects were first discovered by Reuss 1809 [13] from an experimental investigation on porous clay. In 1879, Helmholtz developed the EDL theory, relating the electric and flow parameters for electrokinetic transport. Guoy and Chapman modeled the region near the surface as a diffuse double layer, where they linked the non-uniform ion distribution to the competing electrical and thermal diffusion forces [15]. Stern later presented the basis for the EDL theory, in which the Stern plane splits the EDL into an inner, immobile, compact layer and an outer, diffuse layer.

Earlier studies of EDL and electro-osmotic flows were limited to systems with simple geometries, such as cylindrical capillaries with circular cross sections or slit-type channels formed by two parallel plates [13, 14, 17]. However, the channels in modern microfluidic devices and Micro-Eelectro-Mechanical-Systems (MEMS) are made by microfabrication technologies with cross sections close to rectangular shapes. In such situations, the EDL field is two-dimensional and will affect the two-dimensional flow field in the rectangular microchannel. In the past decade, there have been numerous theoretical [9, 10], numerical [2, 3, 5, 11, 19], and experimental [4, 8] studies on electrokinetic microflows. Almost all of the numerical work just mentioned studied electro-osmotic pumping under steady-state conditions.

To this end, a rectangular microchannel of width, $2W$, height, $2H$, and length, L, is considered to study transient electro-osmotic pumping. With this geometry shown in Fig. 3 both electric potential and velocity fields are symmetric with respect to the channel centerline and the solution domain can be limited to a quarter section of the channel.

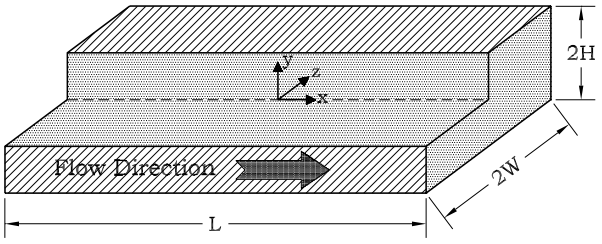

Figure 3. A typical rectangular microchannel

The electric potential distribution due to the presence of an EDL can be described by the non-dimensional Poisson-Boltzmann equation [12],

$$\frac{\partial^2 \psi^*}{\partial y^{*\,2}} + \frac{\partial^2 \psi^*}{\partial z^{*\,2}} = (\kappa D_H)^2 \sinh \psi^* \tag{1}$$

the non-dimensional variables are as follows:

$$\psi^* = \frac{z_e e}{k_B T}\psi \tag{2}$$

$$y^* = \frac{y}{D_H} \quad , \quad z^* = \frac{z}{D_H} \tag{3}$$

where the channel hydraulic diameter, D_H, and the so called Debye-Huckle parameter, κ, are defined as

$$D_H = \frac{2WH}{(W+H)} \tag{4}$$

$$\kappa = \left(\frac{2 n_\infty z_e^2 e^2}{\epsilon \epsilon_0 k_B T} \right)^{1/2} \tag{5}$$

The non-dimensional group, $1/\kappa$, is a measure of the EDL thickness and is often referred to as the electrokinetic diameter. z_e is the valence of the dissolved ions, n_∞ is the ionic number concentration in the bulk solution, e is the fundamental electric charge, ϵ is the dimensionless dielectric constant of the solution, ϵ_0 is the permittivity of vacuum, k_B is Boltzmann's constant, and T is the absolute temperature. Therefore, the EDL thickness depends on the type of dissolved ions, the electrolyte concentration, and the operating temperature.

Equation 1 is subject to the following boundary conditions:

$$y^* = 0 \quad \frac{\partial \psi^*}{\partial y^*} = 0 \quad , \quad z^* = 0 \quad \frac{\partial \psi^*}{\partial z^*} = 0 \tag{6}$$

and

$$y^* = \frac{H}{D_H} \text{ and } z^* = \frac{W}{D_H} \quad \psi = \zeta \text{ or } \psi^* = \frac{z_e e}{k_B T}\zeta = \zeta^* \tag{7}$$

2.2. Velocity Distribution in Rectangular Microchannels

The electro-osmotic pumping efficiency can be obtained with the knowledge of the liquid velocity distribution. The Navier-Stokes equations for a laminar Newtonian liquid flow with constant density, ρ, and viscosity, μ, in a two-dimensional horizontal channel under the influence of an external electric force can be expressed as:

$$\rho\left(\frac{\partial \mathbf{u}}{\partial t}+(\mathbf{u}.\nabla)\,\mathbf{u}\right)=-\nabla P+\mu\nabla^2\mathbf{u}+\mathbf{F} \qquad (8)$$

In the absence of a pressure gradient, liquid flow is induced only by the electrokinetic forces which are assummed to be uniform along the channel. Under these conditions flow is unidirectional and the non-linear advection terms can be dropped out. In other words,

$$v=w=0 \quad \text{and} \quad u=u(y,z,t) \qquad (9)$$

and Eq. 8 is reduced to:

$$\rho\left(\frac{\partial u}{\partial t}\right)=\mu\left(\frac{\partial^2 u}{\partial y^2}+\frac{\partial^2 u}{\partial z^2}\right)+F_x \qquad (10)$$

where F_x is the tangential electric force exerted externally per unit fluid volume. This force is related to the charge density, ρ_e, and electric field strength, E_x as:

$$F_x=\rho_e E_x \qquad (11)$$

The charge density can be expressed in terms of the Boltzmann distribution

$$\rho_e=-2n_\infty z_e e\,\sinh\left(-\frac{z_e e}{k_B}\psi\right) \qquad (12)$$

Since the fluid motion is initiated by the electrical body force (the driving force) acting on the ions in the EDL, electro-osmotic flow depends not only on the applied electrical field but also on the net local charge density in the liquid.

Other non-dimensional parameters are defined to transform Eq. 10 into a dimensionless form as:

$$\frac{\partial u^*}{\partial t^*}=\frac{\partial^2 u^*}{\partial {y^*}^2}+\frac{\partial^2 u^*}{\partial {z^*}^2}+M^* E_x^*\,\sinh\psi^* \qquad (13)$$

where

$$t^*=\frac{\mu t}{\rho D_H^2} \qquad (14)$$

$$u^*=\frac{u}{U} \qquad (15)$$

$$M^*=\frac{2n_\infty z_e e D_H^2}{\mu U L} \qquad (16)$$

$$E_x^*=\frac{E_x L}{\zeta} \qquad (17)$$

Equation 13 is subject to the following initial and boundary conditions

$$t^*=0 \qquad u^*=0 \qquad (18)$$

$$y^*=0 \quad \frac{\partial u^*}{\partial y^*}=0 \quad , \quad z^*=0 \quad \frac{\partial u^*}{\partial z^*}=0 \qquad (19)$$

$$y^*=\frac{H}{D_H} \quad u^*=0 \quad , \quad z^*=\frac{W}{D_H} \quad u^*=0 \qquad (20)$$

The dimensionless group, M^*, in Eq. 16 is the ratio of the electrical to frictional forces per unit volume. Also, a reference velocity, U, is used to nondimensionalize u in the momentum equation. This reference velocity is considered to be equal to 1 mm/s throughout the calculations.

2.3. Solution Method

The EDL equation (Eq. 1) is a nonlinear partial differential equation which must be solved numerically. In the present work, a finite difference scheme with variable grid spacing was developed to discretize the equation. The resulting system of algebraic equations was solved using Gauss-Seidel iterative technique. The resulting electric potential distribution is then substituted into the momentum equation (Eq. 13) which is also solved numerically to obtain the flow distribution in the channel. An Alternating Direction Implicit (ADI) technique combined with the TDMA was utilized to obtain variations of velocity profiles with time.

3 Results and Discussions

Non-dimensional EDL and Navier-Stokes equations were solved simultaneously to identify the characteristics of electro-osmotic flow in a rectangular microchannel. In this section, the effects of different design and operating parameters on electro-osmotic pumping are studied. A dilute KCl solution ($10^{-6}M$) at room temperature was chosen as the working liquid for which ϵ = 80 and μ = 0.0009 $Pa.s$ [18]. The experimentally measured zeta potentials were reported to be 200 mV at this concentration [2].

The non-dimensional EDL profile, $\psi^*(y^*,z^*)$, across a very small corner section of a square channel (D_H = 50

μm) is shown in Fig. 4. Successive grid spacings were reduced by a factor of about 10% to condense the grid sizes in the region near the channel wall, where the EDL effects are most significant. As seen in this figure, the electric potential is maximum at the wall surface and drops off rapidly towards the channel center. In this case, the potential drops to zero within the 10% of W or H. Along the channel diagonal, the thickness of EDL is slightly larger due to the combined effect from both walls. Therefore, the external electric field influences directly on this narrow region. The thickness of this effective region is a strong function of the channel dimension, and the solution concentration as indicated in Eq.1.

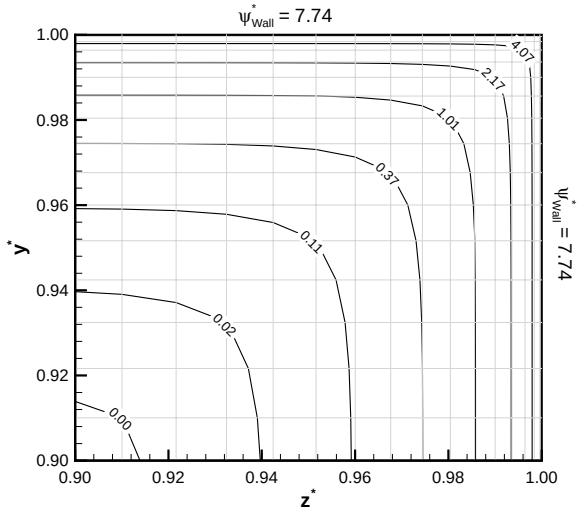

Figure 4. Dimensionless EDL potential in the corner section of a microchannel ($D_H = 50\ \mu m$)

Figure 5a displays the variation of electric potential along the main axes in the same square channel. The resulting velocity profiles are also shown in Fig. 5b as a function of time. As expected, the presence of a large driving force near the channel wall causes the fluid particles to move initially in the EDL. The flow in this region which is induced directly by the electric force can be regarded as the active flow as indicated in the figure. Fluid velocity increases rapidly from zero at the wall (no-slip condition) to a maximum near the wall, and then gradually drops off due to significant reduction in the EDL strength. As time elapses, momentum is continuously transferred from the active layers to the central fluid until a steady-state flow is attained. The passive flow in the channel center, which is caused by viscous drag forces, has a lower velocity compared with the active flow near the wall. As seen from the figures, it takes a

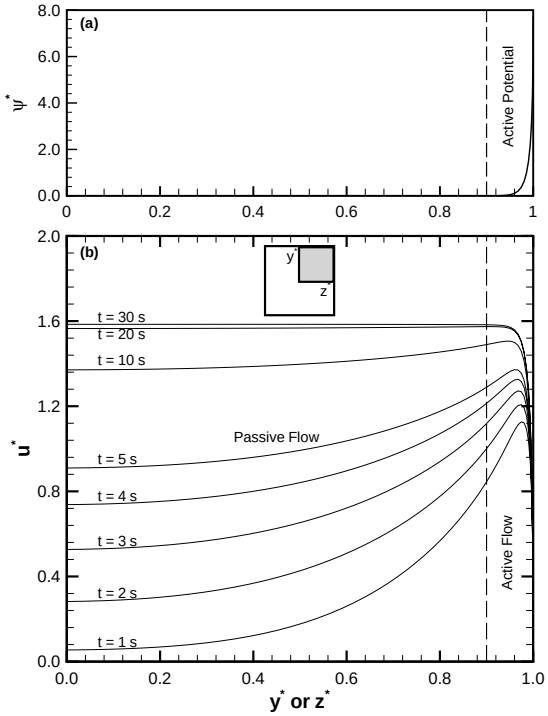

Figure 5. Transient velocity profile along the main axes of a square channel($D_H = 50\ \mu m, \Delta E = 100\ V$)

relatively long time (about 30 s) for the flow to reach steady state.

Figure 6 shows time variations of 3-D flow fields. The contour plots clearly indicate the inception of a maximum velocity in the channel corner and its evolution towards the central areas. Numerical results have shown that the flow velocity in the channel corner is always maximum during the transient periods for all hydraulic diameters examined.

It is very useful to express the performance of electro-osmotic pumping in terms of the volumetric flow rates. Total flow rates can be calculated by integrating velocity distributions across the channel area as follows:

$$Q = 4 \int_0^H \int_0^W u(y,z)\,dz\,dy \tag{21}$$

In the following sections, effects of design and operating parameters on the transient and steady state flow fields in a microchannel will be studied.

3.1. Effect of Hydraulic Diameter

Hydraulic diameter has a strong effect on the transient and steady state electro-osmotic pumping in microchan-

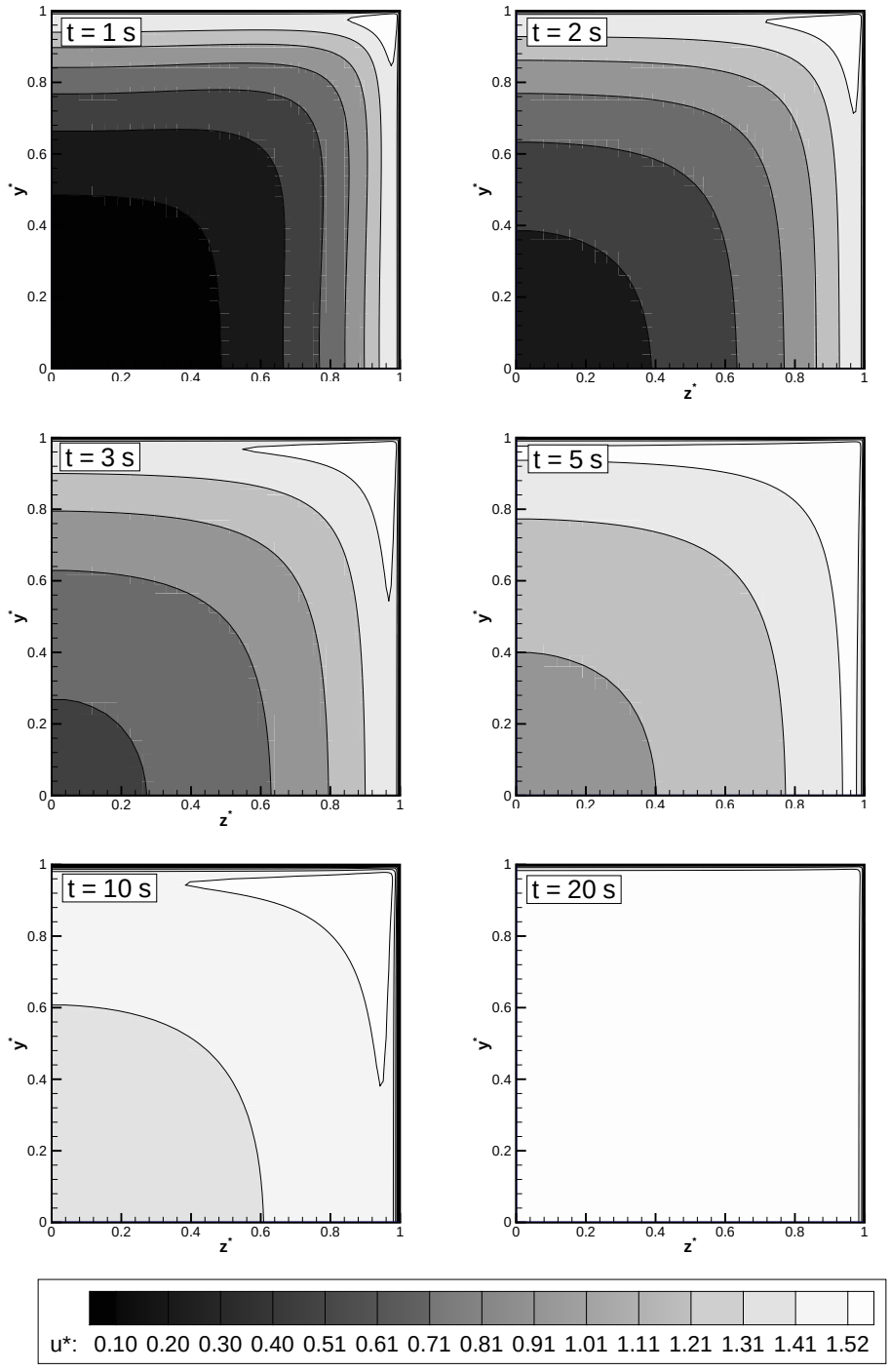

Figure 6. Transient 3D velocity distributions in a square channel ($D_H = 50\ \mu m, \Delta E = 100\ V$)

nels. Hydraulic diameter not only affects the EDL thickness (κD_H), but also influences the strength of the viscous forces (M). Figure 7a shows time variations of volumetric flow rate as a function of channel hydraulic diameter. As shown in the figure, steady-state flow is maintained almost immediately in the microchannels with small hydraulic diameters (*e.g.* $10 \sim 20\ \mu m$). This is mainly because the momentum has to penetrate into a very short distance. As the hydraulic diameter is increased, a larger flow rate is obtained at the cost of a longer transient time. This is an important issue for applications in which a controlled flow delivery is required. Figure 7b also shows that as the channel hydraulic diameter is increased, the average velocity is decreased.

3.2. Effect of Aspect Ratio

Design and fabrication flexibilities are among the important concerns in microfluidic systems. One parameter of interest in this category is the height-to-width ratio or simply the cross sectional area aspect ratio, AR. With a rectangular microchannel not only the hydraulic diameter influences the velocity profile but also the aspect ratio may have a significant effect on the potential and flow fields.

The effect of the aspect ratio on the flow field and the channel throughput will be investigated in this section. At constant cross sectional areas (1,600 $\sim$ 10,000 μm^2), the aspect ratio, W/H, has been changed incrementally from square (1:1) to 1:10 to study its effect on the transient and steady state flow rates.

The volumetric flow rate in a microchannel with a cross sectional area of 2500 μm^2 is shown in Fig. 8. As shown in this figure, when the aspect ratio is decreased, the steady state flow field prevails in a shorter time. In addition a slightly larger flow throughput is attained under steady state conditions. This is again due to the smaller penetration depth for the momentum, which is transferred from the wall towards the channel center as pointed out, earlier.

The effect of aspect ratio on the channel throughput for other cross sectional areas shows a similar trend. A summary of steady state flow rates and the percentage of increase in flow rates are given in Table 1. The numerical results clearly indicate that by decreasing the aspect ratio, the flow throughput is increased regardless of the cross sectional area however, the aspect ratio effect is the strongest for smaller areas.

Numerical simulations showed that the channel orientation has no effect on the channel throughput. This is in agreement with the results reported by Arulanandam and Li (2000) [2].

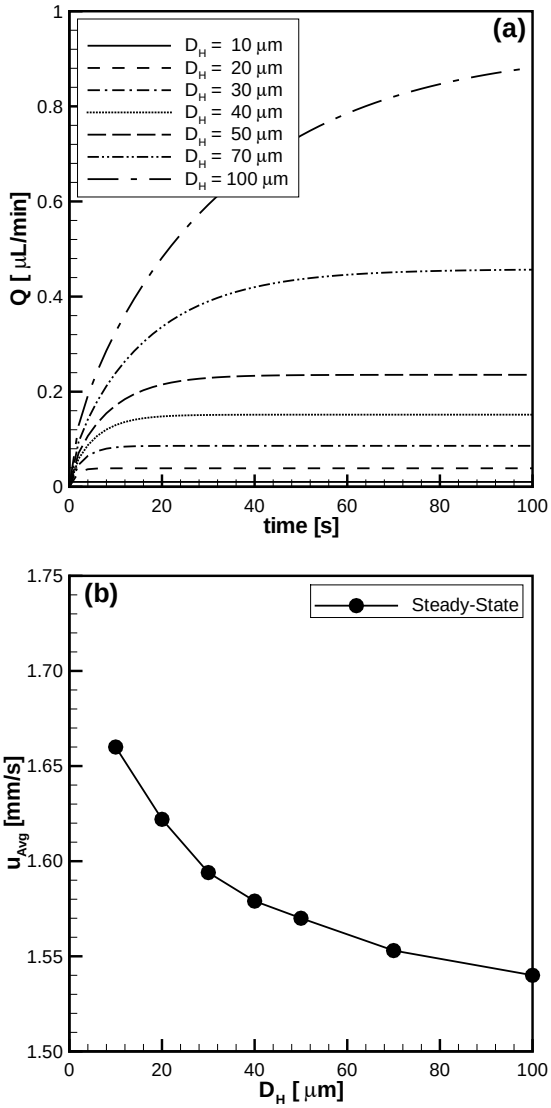

Figure 7. Effect of the channel hydraulic diameter on (a) transient volumetric flow rate and (b) on the steady state average velocity ($\Delta E = 100\ V$)

3.3. Effect of Electric Field Strength

Electro-osmotic flow, as explained earlier, is the result of a tangentially applied electric field on a channel in the presence of an EDL. A direct relationship exists between the applied voltage and the flow velocity as shown in the governing equations. Thus, with all other parameters held constant, there should be a linear variation in volumetric

Table 1. Effect of AR on the steady state flow rates in microchannels ($\Delta E = 100\ V$)

AR (H/W)	$1,600\mu m^2$ Q $[\mu L/min]$	Change [%]	$2,500\mu m^2$ Q $[\mu L/min]$	Change [%]	$4,900\mu m^2$ Q $[\mu L/min]$	Change [%]	$10,000\mu m^2$ Q $[\mu L/min]$	Change [%]
1/10	0.1633	7.6	0.2509	6.5	0.4809	5.3	0.9575	4.9
1/6	0.1601	5.5	0.2461	4.5	0.4719	3.3	0.9463	3.7
1/4	0.1566	3.2	0.2419	2.7	0.4673	2.3	0.9392	2.9
1/2	0.1532	1.0	0.2375	0.9	0.4601	0.8	0.9246	1.3
Square	0.1517	—	0.2355	—	0.4566	—	0.9124	—

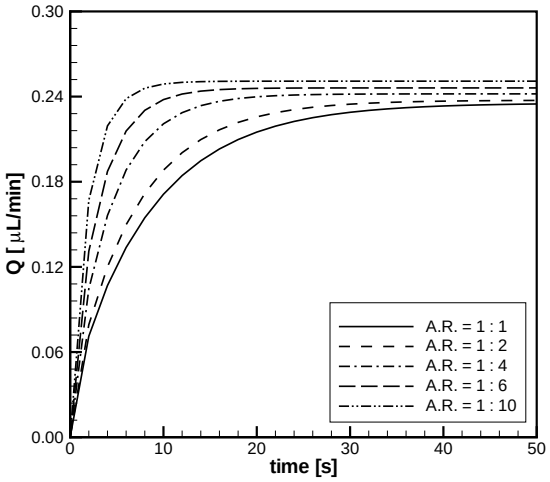

Figure 8. Effect of aspect ratio on the transient behavior of the microchannel ($\Delta E = 100\ V$)

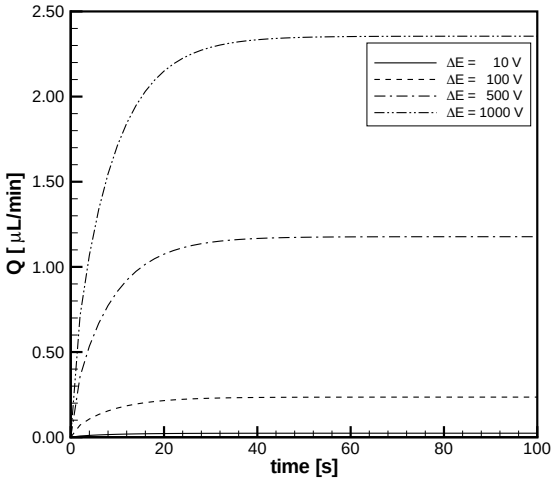

Figure 9. Effect of applied voltage on the transient and steady state flow in microchannel ($D_H = 50\ \mu m$)

flow rate with the applied voltage along the microchannel. This linear dependence has been experimentally observed for electric fields strengths of up to $3 \times 10^7\ V/m$ [16].

Figure 9 shows the effect of applied voltage on the transient and steady state flow through a microchannel with a square cross sectional area (D_H = 50 μm). It is observed that the steady state flow is increased linearly with the applied voltage. So, when larger pumping flow rates are required, larger voltages would seem to be a better choice. However, this is always a limitation for portable micro systems. In addition, the higher electric field strengths may lead to an increase in fluid temperature as pointed out earlier.

4. Conclusions

Two-dimensional Poisson-Boltzmann and momentum equations were solved simultaneously to study the transient characteristics of electro-osmotic pumping in a rectangular microchannel. Numerical solutions show significant influences of the channel hydraulic diameter, the aspect ratio, and the applied voltage on the volumetric flow rates under transient and steady state conditions. As the channel hydraulic diameter is increased, it takes a longer period for the flow to become steady state. On the other hand, as the channel aspect ratio deviates from the square, a steady-state flow field is reached in a shorter period, and a slightly larger flow can be obtained. This is an important finding for microfluidic systems with large hydraulic diameters operating

under unsteady conditions. The numerical results also show that the steady state channel throughput is linearly increasing with the applied voltage along the channel length.

5. Nomenclature

D_H	hydraulic diameter $[m]$
e	fundamental electric charge $[1.60217733^{-19}\ C]$
E	electric field strength $[V/m]$
F	force $[N]$
H	channel half height $[m]$
k_B	Boltzmann constant $[1.381 \times 10^{-23}\ J/K]$
L	channel length $[m]$
M	dimensionless group defined in Eq. 16 [ ]
n_∞	bulk ionic number concentration $[m^{-3}]$
P	pressure $[Pa]$
Q	volumetric flow rate $[m^3/s]$
T	temperature $[K]$
u	velocity $[m/s]$
U	reference velocity $[m/s]$
V	voltage $[V]$
W	channel half width $[m]$
x	x-direction $[m]$
y	y-direction $[m]$
z	z-direction $[m]$
z_e	valance of the dissolved ions [ ]

Greek Letters

ϵ	dimensionless dielectric constant [ ]
ϵ_0	permittivity of vacuum $[8.85 \times 10^{-12}\ C^2/N.m^2]$
ζ	zeta potential $[V]$
κ	dimensionless group defined in Eq. 5
μ	viscosity $[Pa.s]$
ρ	density $[kg/m^3]$
ψ	potential $[V]$

References

[1] A. Adamson and A. Gast. *Physical Chemistry of Surfaces*. John Wiley and Sons, New York, NY, 1997.

[2] S. Arulanandam and D. Li. Liquid transport in rectangular microchannels by electro-osmotic pumping. *Colloids and Surfaces A: Physiochemical and Engineering Aspects*, 161:89–102, 2000.

[3] F. Bianchi, A. Ferrigno, and H. Girault. Finite element simulation of an electro-osmotic-driven flow division at a t-junction of microscale dimensions. *Anal. Chem.*, 72(9):1987–2000, 2000.

[4] C. Culbertson, R. Ramsey, and J. Ramsey. Selective ion transport using electrokinetic pumps on microchips. *Anal. Chem.*, 72(10):2285–2291, 2000.

[5] S. Ermakov, S.V.and Jacobson and J. Ramsey. Computer simulations of electrokinetic transport in microfabricated channel structure. *Anal. Chem.*, 70:4494–4504, 1998.

[6] M. Gad-el Hak. *The MEMS Handbook*. CRC Press, 2002.

[7] R. Hunter. *Zeta Potential in Colloid Science*. Academic Press, London, 1981.

[8] S. Jacobson, T. McKnight, and J. Ramsey. Microfluidic devices for electrokinetically driven parallel and serial mixing. *Anal. Chem.*, 71:4451, 1999.

[9] H. Keh and Y. Liu. *J. Colloid Interface Surf.*, 172:222–229, 1995.

[10] H. Ohshima and T. Kondo. Electrokinetic flow between two parallel plates with surface-charge layers-electro-osmosis and streaming potential. *Colloid Interface Sci.*, 135(2):443–448, 1990.

[11] N. Patankar and H. Hu. Numerical simulation of electro-osmotic flow. *Anal. Chem.*, 70:1870–1881, 1998.

[12] R. Probstein. *Physiochemical hydrodynamics: An introduction*. Wiely and Sons, New York, NY, 1994.

[13] F. Reuss. Memorires de la societe imperiale de naturalistes de moscou. 3:327, 1809.

[14] C. Rice and R. Whitehead. Electrokinetic flow in a narrow cylindrical capillary. *J. Phys. Chem.*, 69:4017–4023, 1965.

[15] D. Shaw. *Electrophoresis*. Academic Press, New York, 1969.

[16] P. Vincett. *J. Coll. Int. Sci.*, 69:354, 1979.

[17] M. von Smoluchowski. Studien ber molekularstatistik von emulsionen und deren zusammenhang mit der brownschen bewegung. *Wien Berichte*, 123:2381–2405, 1914.

[18] R. Weast, M. Astle, and W. Beyer. *CRC Handbook of chemistry and physics*. CRC Press, Boca Raton, 2001.

[19] C. Yang, D. Li, and J. Masliyah. Modeling forced liquid convection in rectangular microchannels with electrokinetic effect. *Int J. Heat and Mass Trans*, 41:4229–4249, 1998.